2018/6/25Rare Metal Materials and Engineering
Volume 47, Issue 6, June 2018
Online English edition of the Chinese language journal

Available online at www.sciencedirect.com
ScienceDirect

Cite this article as: Rare Metal Materials and Engineering, 2018, 47(6): 1677-1681.

ARTICLE

Formation and Properties of Porous ZrO_2-8wt%Y_2O_3 Coatings

Ding Kunying[1, 2], Cheng Taotao[2], Han Zhiyong[2]

[1] Tianjin Key Laboratory for Civil Aircraft Airworthiness and Maintenance, Civil Aviation University of China, Tianjin 300300, China; [2] College of Science, Civil Aviation University of China, Tianjin 300300, China

Abstract: The efficiency of a gas turbine engine is highly dependent upon the clearance between blades and engine case. To control the over-tip leakage, an abradable coating system is sprayed on the case surface. In the high temperature section, a ZrO_2-8wt%Y_2O_3 (YSZ) coating is usually applied. Pores in the coating enhance its abradability. In this study, poly-p-hydroxybenzoate (PHB) powder mixed in the YSZ powder was used as pore-forming material. To avoid burning loss of PHB during the spraying process, a sol-gel method was used to clad a TiO_2 shell on the PHB powder surface. The porous YSZ coating was deposited by plasma spraying. The characteristics of the coatings were investigated in this work, such as morphology, porosity, hardness, corrosion resistance and abradability. The results show that the coated PHB increases the porosity of the YSZ coating, and then decreases the coating hardness. Finally, a rotated invading test indicates the incursion depth increases with the increase of coating porosity, suggesting the coating abradability is improved.

Key words: ZrO_2-8wt%Y_2O_3; abradability; sol-gel; porosity; incursion depth

As previous research works report, the efficiency of a gas turbine engine can be increased by minimizing the clearance between rotating and stationary parts[1]. To reach this aim, an abradable seal coating is used to be deposited on the inner wall of the engine casing via plasma spraying[2]. As the turbine blade rotates at around 10 000 r/min, the blade tip may incur into the seal coating to close the gap between the blade tip and shroud. Once the seal coating is used in the high temperature section, a ceramic-based coating such as ZrO_2-8wt%Y_2O_3 (YSZ) is commonly applied for its superior thermal barrier property[3,4]. As a kind of seal coatings, the ceramic coating should be soft enough to avoid a significant blade wear, thus allowing much smaller clearances.

According to previous works, the coating hardness was affected by the porosity, which could be adjusted to achieve the abradable function of the coatings [5,6]. Generally, the porosity of YSZ coatings is below 10%, which is too low to achieve the purpose of adjustment. Nicoll[7] invented a new YSZ coating deposited by hollow powder to increase the porosity to around 30%. However, the high cost kept this coating from extensive application. Sanjuán [8] blended polymers such as poly-p-hydroxybenzoate (PHB) with YSZ powder stocks to increase coating porosity to around 20%. This is a low cost approach to increase coating porosity. However, PHB has a tendency to decompose during the spaying process due to the high plasma temperature, resulting in an instable coating porosity, which substantially bring about blade ab rasion.

To decrease PHB decomposing, a layer of TiO_2 was clad on PHB to avoid it contacting with the plasma directly in this paper. Therefore, the porosity of the coating could be increased steadily, resulting in an improved abradability.

1 Experiment

Three kinds of powder feedstock were tested: (A) agglomerated pure YSZ powder, (B) agglomerated YSZ with mixed uncoated PHB, and (C) agglomerated YSZ with mixed coated PHB. As a raw powder, the PHB mixed in the agglomerated powders take a decisive effect in increasing coating porosity[9]. For comparison, powder B and C contained the same amount

Received date: June 14, 2017
Foundation item: National Natural Science Foundation of China (51501222); Civil Aviation Science and Technology Project (MHRD20160106); Fundamental Research Funds for the Central Universities (3122015L001)
Corresponding author: Ding Kunying, Ph. D., Lecturer, College of Science, Civil Aviation University of China, Tianjin 300300, P. R. China, Tel: 0086-20-24092074, E-mail: dingkunying@126.com

of PHB. The flowability and apparent density of the agglomerated powder were investigated by a FL4-1 hall flow meter. Their components and properties are listed in Table 1. Fig.1a shows the morphology of the PHB powder with a particle sizes of 10~25 μm. A smooth powder surface and near-spherical morphology are observed. In order to enhance the thermal resistance of this powder, a new approach of sol-gel procedure was used. PHB powder was mixed into the tetrabutyl titanate-ethanol solution under magnetic stirring conditions. Titania sol and gel were generated by dripping acidic water in the solution. Then PHB coated with titania emerged after dying and milling. After sieving, the coated powder had a particle size between 10 μm and 25 μm. The morphology of the coated PHB powder is shown in Fig.1b. Polygonal and fine particles are observed on the PHB surface, forming a shell to avoid PHB contacting plasma directly[10,11].

The un-coated PHB or as-received coated PHB, YSZ raw powder with a particle sizes of 2~10 μm and some polyvinyl alcohol (PVA) were dispersed in deionized water by a ball-milling machine, to make the slurry for agglomeration. The agglomerated powders were then fabricated by spray dying in the tower at 300~320 °C intake temperature and 100~120 °C outlet temperature with the atomizer rotating at 1800 r/min. The final powders A, B and C with a particle sizes of 45~106 μm were selected for plasma spraying.

Table 1 Components and properties of the powder feedstock

Powder	Composition/wt%			Apparent density/ g·cm^{-1}	Flowability /s·50 g^{-1}	Particle size/μm
	YSZ	PHB	Coated-PHB			
A	100	-	-	1.58	21.2	45~106
B	90	10	-	0.86	38.3	45~106
C	86.8	-	13.2	0.92	31.7	45~106

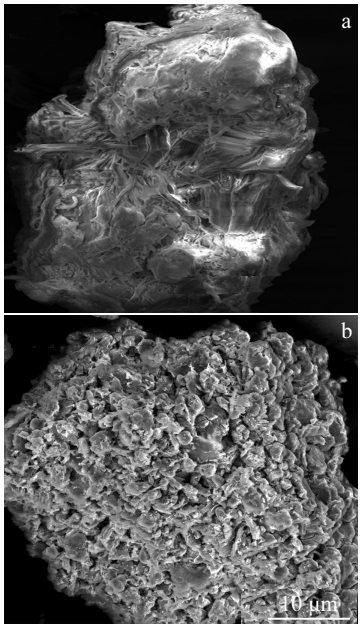

Fig.1 Morphologies of PHB (a) and coated PHB (b) particle

The specimens were made by a Ni718 alloy, and were cleaned by acetone and sandblasted by alumina. In order to enhance the bond strength of the ceramic coating, a metal coating of CoNiCrAlY was deposited on the substrate surface firstly. Then the agglomerated powders of Powder A, B, C were sprayed using Praxair 3710 plasma equipment to form Coating A′, B′, C′, respectively. The thickness was around 250 μm for the top coating and around 100 μm for the bond coating. The optimized spraying parameters are listed in Table 2. The finish coated specimens were heated at 550 °C for 2 h in the furnace to generate pores through a decomposition process of the PHB[12].

The morphology of the powders and microstructure of the coating cross-sections were analyzed by a scanning electron microscope (QUANTA-200 FEI, Netherlands). An image analyzer based on gray contrast was used to determine mean coating porosity. A superficial Rockwell hardness tester (TH320, TME, USA) with an indent load of 147 N was used to examine the superficial hardness of the top coatings. To estimate the corrosion resistance of the specimens, potentiodynamic polarization curves were obtained via an electrochemical workstation (P4000, PRINCETON,USA) in 3.2 wt% sterile seawater. The experiment was conducted in a standard three-electrode system with the tested specimen as a working electrode, the Pt net as a counter electrode and the saturated calomel electrode as a reference electrode. Before electrochemical tests, the specimen was immersed in the sterile seawater for 30 min to ensure the steady state.

Ni718 alloy samples coated with the coating system obtained above (100 μm bond coating, 250 μm top coating) were used as samples for abradability rig testing (Fig.2). A bearing steel pin with HRC 55 hardness was pressed on the coating surface with a pressure of 40 N, and then rotated at a speed of 20 m/s. According to the incursion rate, the test endured in a 200 s period. The gross mass loss of the pin was measured by an electronic balance with the accuracy of 0.001 g. The cross-sections of the abraded coating samples were analyzed by a laser microscopy (OLYMPUS-OLS4100, Japan).

2 Results and Discussion

Three kinds of top coatings (coating A′ sprayed by powder A,

Table 2 Spraying parameters for the top and bond coatings

Powder	Current/A	Voltage/V	Spraying distance/mm
CoNiCrAlY	780	38	85
A	850	40	75
B	850	40	75
C	850	40	75

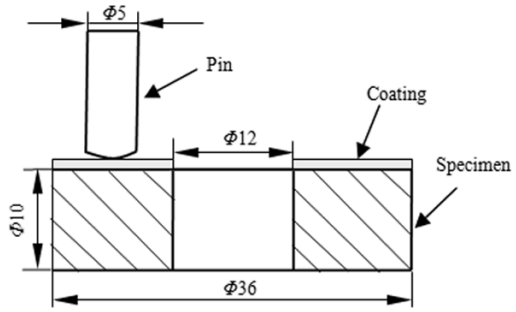

Fig.2 Schematic diagram of the abrasive rig (mm)

coating B′ sprayed by powder B and coating C′ sprayed by powder C) were deposited on CoNiCrAlY bond coating. The cross-section micrographs of the coating are shown in Fig.3. Different pore morphology and distribution are exhibited in the top coatings. Coating A′ possesses the lowest porosity in the current coatings at about 3.3%. The mean pore size of coating A′ is approximately 7 μm. The mean porosity increases to 11.5% in coating B′ and the mean pore size increases to about 17 μm as a result of the emergence of some larger pores due to mixed PHB. Finally, the mean porosity and pore size increase to 23.5% and 20.5 μm, respectively in coating C′, because of remarkable increase of larger pores.

The microstructure of larger pores in coating C′ was analyzed by the SEM, as shown in Fig.4a. Based on energy spe trum, the elements of Zr, Y and O were detected in the top coating, indicating the components of this coating (Fig.4b). And the elements of Ti and O were detected around the boundary of the pores (Fig.4c), indicating the TiO_2 shell deposited on the PHB has been retained in the coatings. The TiO_2 shell can prevent the PHB from directly contacting with plasma arc during the spraying process so that more PHB would remain to generate higher porosity through subsequent decomposition.

As shown in Table 3, the superficial hardness decreases with the increase of coating porosity. The pores presented in coatings decrease the stressed area when the indenter is pressed on the surface, resulting in a decline in hardness[13-18]. So it can be concluded that more pores induce lower hardness.

The anti-corrosion behavior of the bare Ni718 and the alloy with coating A', B', C' were characterized by potentiodynamic polarization curves and corrosion current densities (I_{corr}) in Fig.5.

The corrosion rate could be calculated by corrosion inhibition efficiency (E_I) in Eq.(1) [19]

$$E_I=(I_a-I_b)/I_a \quad (1)$$

where I_a and I_b are referred to the corrosion current densities of sample a and sample b, respectively. This equation reveals that

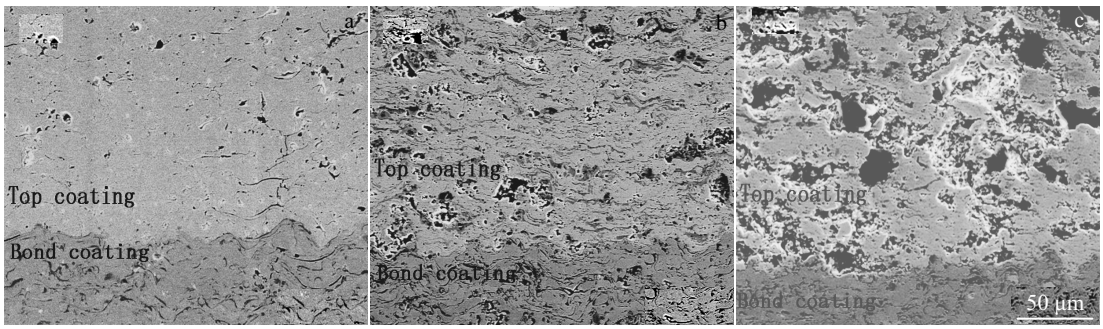

Fig.3 Cross-section morphologies of coating A′ (a), coating B′ (b), and coating C′ (c)

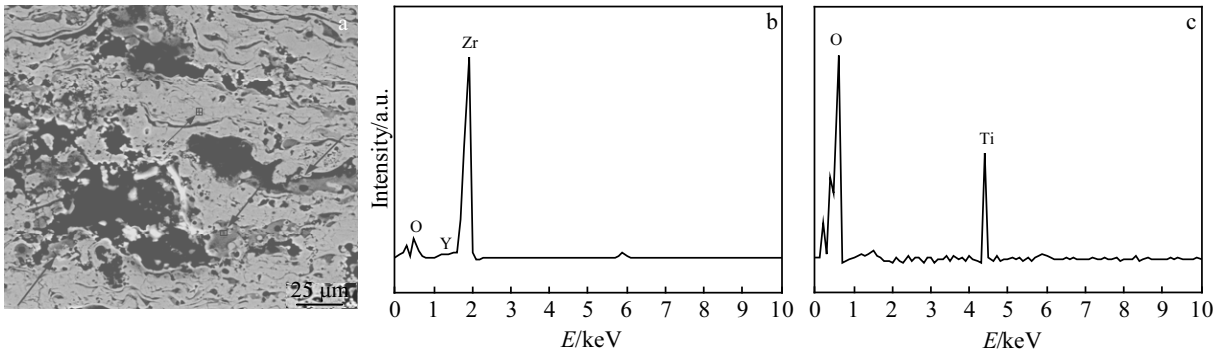

Fig.4 Microstructure of larger pores in coating C′ (a), EDS spectrum of the top coating (b), and EDS spectrum of the gray area around the large pores (c)

Table 3 Mechanical properties of different coatings

Coating	Mean porosity/ %	Mean pore size/ μm	Superficial hardness/ HR_{15y}
A′	3.3	7.2	96.4±8.4
B′	11.5	17.1	82.5±9.6
C′	23.5	20.5	68.7±8.5

Table 4 Abradable properties of different coatings

Coating	Load/ N	Rotation speed/r·min^{-1}	Pin mass loss/mg	Max incursion depth/μm
A′	40	1200	12	10.8
B′	40	1200	7	87.3
C′	40	1200	3	244.6

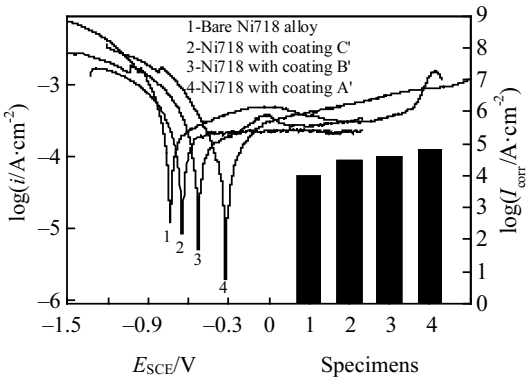

Fig. 5 Potentiodynamic polarization curves and corrosion current densities of bare Ni718 and specimens with different coatings

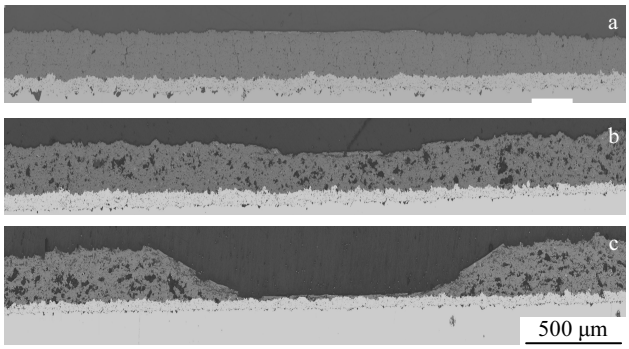

Fig.6 Cross-section micrographs of the worn samples with coating A′ (a), coating B′ (b), and coating C′ (c)

E_I of the specimens with the coating A', B', and C' compared with bare Ni718 is 80.2%, 73.5%, 51.6%, respectively. It is obvious that the coatings promote the corrosion resistance of Ni718 alloy, and the corrosion current densities decrease with the increasing of coating porosities.

For evaluating the abradability of applied coatings, the underlying principle is similar for the different test rig configurations. A dummy blade is used to run against a coated specimen with a certain pressure and at a certain rotation speed[20,21]. The mass loss of the dummy blade and the incursion depth of the coating can be used to evaluate the abradability of the coatings. In this experiment, a pin with blunt tip was used to simulate the blade, pressed on the coating with a 40 N pressure and then rotated at a 20 m/s speed. The abradability test results are summarized in Table 4. As the rotating pin was pressed on the coating A′ surface, it presented very serious wear at the tip. Meanwhile, the surface of coating A′ demonstrated an anti-incursion capability. The mass loss of the pin is 12 mg and the maximum incursion depth of the coating is only 10.8 μm after 200 s test. Coating B′ illustrates a better abradable property with a pin mass loss of 7 mg and a maximum incursion depth of 87.3 μm. For coating C′, the pin mass loss decreases to 3 mg, and the coating incursion depth increases rapidly to 244.6 μm.

The cross-section micrographs of the invaded samples deposited with coating A′, B′ and C′ are shown in Fig.6. A low incursion depth and a smooth surface are found at the abrasion area of coating A′. And the coating cross-section exhibits many cracks with some new propagation due to the effect of incursion, as shown in Fig.6a.

A larger incursion depth and fewer cracks are shown in coating B′ (Fig.6b) than in coating A′. For coating C′, the area invaded by the rotate pin is abraded off completely, but the other area is retained as a well structure, as shown in Fig.6c.

In current coatings, coating C′ exhibits the best abradability due to the increased porosity and appropriate pore distribution. At the incursion situation, pores promote the crack connection in the abrasion area, bring in an increase of coating wear rate, and then improve the coating abradability.

3 Conclusions

1) The porosity of the top coating increases to 11.5% from 3.3% after directly mixing 10 wt% PHB into the YSZ powder. Once a TiO_2 layer is deposited on the PHB surface before mixing, the porosity increases to 28.5%.

2) The superficial hardness of the top coating presents an obvious decrease as the porosity increases.

3) The lower hardness of the top coating induces a lower mass loss of the rotate pin and a deeper incursion depth of the top coating during the abradability test.

References

1 Chupp R E, Ghasripoor F, Turnquist N A *et al*. *Journal of Propulsion and Power*[J], 2002, 18(6): 1260

2 Novinski E, Harrington J, Klein J. *Thin Solid Films*[J], 1982, 95(3): 255

3 Heveran C M, Xu J P, Sarin V K *et al*. *Surface & Coating Technology*[J], 2013, 235: 354

4 Keyvani A, Saremi M, Sohi M H *et al*. *Journal of Alloys and Compounds*[J], 2014, 600: 151

5 Bardi U, Giolli C, Scrivani A *et al*. *Journal of Thermal Spray*

Technology[J], 2008, 17: 805
6 Arai M, Suidzu T. *Journal of Thermal Spray Technology*[J], 2013, 22: 690
7 Dai H, Wang L M, Zhang J P *et al*. *Materials Review*[J], 2008, 22(7): 18 (in Chinese)
8 Sanjuán M L, Oliete P B, Várez A *et al*. *Journal of the European Ceramic Society*[J], 2012, 32: 689
9 Richardt K, Bobzin K, Sporer D *et al*. *Journal of Thermal Spray Technology*[J], 2008, 17: 612
10 Gunji S, Shimotsuma Y, Miura K. *Journal of Sol-Gel Science and Technology*[J], 2016, 79: 151
11 Bumajdad A, Madkour M, Abdel-Moneam Y *et al*. *Journal of Materials Science*[J], 2014, 49: 1743
12 Faraoun H I, Grosdidier T，Seichepine J L *et al*. *Surface & Coating Technology*[J], 2006, 201: 2303
13 Deng C, Liu M, Wu C *et al*. *Journal of Thermal Spray Technology*[J], 2007, 16: 604
14 Shi H, Zhao C Y, Wang B X. *Ceramics International*[J], 2016, 42: 10 184
15 Seuba J, Deville S, Guizard C *et al*. *Science and Technology of Advanced Materials*[J], 2016, 17: 128
16 Gao Y, Gao J Y, Yang D M. *Advanced Engineering Materials*[J], 2014, 16: 406
17 Madhwal M, Jordan E H, Gel M. *Materials Science and Engineering A*[J], 2004, 384: 151
18 Chicot D, Demarecaux P, Lesage J. *Thin Solid Films*[J], 1996, 283: 151
19 Li X W, Zhang Q X, Guo Z *et al*. *Applied Surface Science*[J], 2015, 342: 76
20 Hardwicke C U, Lau Y C. *Journal of Thermal Spray Technology* [J], 2013, 22: 564
21 Ma X, Matthews A. *Surface & Coating Technology*[J], 2007, 202: 1214

多孔 ZrO_2-8%Y_2O_3 涂层的制备及性能

丁坤英[1,2]，程涛涛[2]，韩志勇[2]
(1. 中国民航大学 天津市民用航空器适航与维修重点实验室，天津 300300)
(2. 中国民航大学 理学院，天津 300300)

摘　要：航空发动机的效率与转动叶片和机匣之间的间隙密切相关。为了控制转子和静子之间的间隙，需要在机匣表面制备耐磨耗的封严涂层。在发动机的高温端，ZrO_2-8%Y_2O_3(质量分数) 涂层是经常采用的封严涂层基体。涂层中的孔隙可以增加涂层的耐磨耗性。利用聚苯酯（PHB）增加等离子喷涂的 ZrO_2-8%Y_2O_3 涂层的孔隙率。为了避免聚苯酯在等离子喷涂过程中的烧损，利用溶胶-凝胶法在聚苯酯颗粒表面沉积一层 TiO_2 层。讨论采用此方法制成的涂层的形态、孔隙率、硬度和耐磨耗性。结果表明，在喷涂粉末中混合包覆型的聚苯酯后，涂层的孔隙率得到提升，涂层硬度下降。磨耗试验的结果表明涂层的磨耗深度随着涂层孔隙率的增加而增加。

关键词：ZrO_2-8% Y_2O_3；耐磨耗性；溶胶凝胶；孔隙率；磨耗深度

作者简介：丁坤英，男，1981 年生，博士，讲师，中国民航大学理学院，天津 300300，电话：022-24092074，E-mail: dingkunying@126.com